

PREDICTION OF DEGRADATION IN 90° ELBOW JOINTS OF BA35 BRASS USED IN POTABLE WATER PIPES THROUGH COMPUTATIONAL FLUID DYNAMICS (CFD) SIMULATION

H.T. Bennis¹, H. Zniker^{1,2*}, M.K. El Kouifat¹, M. Bennajah³ and B. Ouaki¹

¹Department of Materials Engineering, The National Higher School of Mining of Rabat (ENSMR), MOROCCO

²Laboratory of Material Physics and Subatomic, Faculty of Sciences, Ibn Tofail University, BP 133, MOROCCO

³Industrial Process Engineering, The National Higher School of Mining of Rabat (ENSMR), BP: 753 Agdal-Rabat, MOROCCO

E-mail: zniker.houcine@gmail.com

Failure of 90° elbows in water pipes due to corrosion is a critical issue in water supply and distribution systems. Therefore, understanding the behavior of pipelines under corrosion is essential to increase their durability. This original study aims to specifically analyze the failure of 90° elbows due to the erosion-corrosion phenomenon. The behavior of water flow, in terms of velocity profile, pressure gradient, and turbulence zones at these elbows, is numerically simulated using the computational fluid dynamics (CFD) method. The simulations, performed with FLUENT software, identify the areas most susceptible to erosion and corrosion, thus contributing to a better understanding of processes such as stress corrosion cracking and cavitation. This work also highlights the importance of designing elbows with suitable characteristics and adopting adequate maintenance practices to prevent failures. These results can serve as a basis for future experimental validations and for the design of more robust pipeline systems.

Key words: potable water pipelines, CFD, corrosion, erosion.

1. Introduction

One of the biggest challenges facing potable water distribution systems is the long-term forecast of metal component degradation, especially damage from corrosion. These kinds of damage are especially likely to affect curved parts, such as elbow joints, which can seriously impair the functionality of water pipelines. A thorough understanding of these components' behavior, when subjected to water flow, erosion, and corrosion, is crucial due to the potential risk associated with such degradation [1-3].

Several authors have investigated experimentally the erosion wear and the combined erosion-corrosion in 90° elbows to collect practical data on these phenomena [4-6]. Zeng *et al.* [7] observed that degradation at the external curvature of 90° elbows is worse than that at the internal curvature in liquid-sand flows, and the erosion increases as the fluid progresses downstream. Owen *et al.* [8] have recently developed 90° elbow geometry to investigate erosion-corrosion loss of carbon steel and found that such geometry was more damaging to the material. Kesana *et al.* [9] discussed effect of erosive particle size/diameter and viscosity of carrier fluid on the wear rate in multiphase flow systems with plane 90° elbows. Vieira *et al.* [10], in a number of tests, also indicated that the orientation of the elbow enhances the degree of impact as well as the erosion rates. Last of all Parsi *et al.* [11] conducted a numerical investigation on plug flow erosion using sand particles in 90° elbows and it was found that the maximum erosion happened at the top of the elbow if it is in the horizontal position.

* To whom correspondence should be addressed

The erosion mechanism of the 90° elbows is a very complex process that depends on the fluid properties and the characteristics of the particles that impinge on the elbow including their shape, size, material, impact velocity and angle of incidence [12-14]. Prediction of particle erosion on pipe walls is one of the major challenges.

Computers and increasing computational power made the use of computational fluid dynamics (CFD) as a tool to produce fluid flow solutions with or without performing solid-solid interactions widespread [10]. CFD is a process in which physical phenomena involving fluid flow are modeled mathematically and solved numerically using computing power [15-17]. CFD has been tested as being effective method in solving practical problems and is widely used in many industries. Hence, over the course of the past years CFD techniques have emerged as one of the primary approaches to analysing flow phenomenon [18].

Therefore, several researchers have investigated erosion of pipelines under various operating conditions through CFD approach by simulations [19, 20]. This remains as the most significant benefit when using CFD-based erosion analysis since several factors causing corrosion can be assessed separately or collectively to determine areas prone to severe material erosion. Moreover, this method can determine the maximum erosion rate for complex shapes of the geometrical structures, which are not easy to study through experiments. Peng *et al.* [21] numerically studied erosion in a water pipe bend with helps of the turbulent flow model, the DPM model and the E/CRC erosion model as well as the particle-wall rebound model. It can be seen from the result that the erosion rate rises with the flow rate, the mass flow rate and the bend angle, but reduce with the pipe diameter or R/D ratio. Furthermore, as the particle size increases, the erosion rate is found to decrease first and then increase to a minimum of $150 \mu\text{m}$ particle size. Ejeh *et al.* [22] employed the RAS and PTM for the modeling of fluid flow and particle tracking in a 45° , 90° , 135° and 180° crude oil pipeline bends. It has been found out that the erosion rate is relatively higher at the bends and the maximum erosion zone is dependent on curve of the pipe. Furthermore, the erosion rate is influenced by particle velocity, mass and density: it also emerged that the larger these parameters, the higher the estimated rate of river bank erosion. Laín *et al.* [23] studied the erosion in 90° pipeline bends using Euler-Lagrange method and Oka erosion model with various factors in to consideration. According to papers cited by Hussein, their investigations establish that with the enhancement of the wall roughness the erosion rate drops sharply and in the case of the larger particles the mean erosion rate is increased. Also, the mass flow rate of the particles has been found to affect the erosion rate where the rate of erosion reduces as the mass flow rate of the particles increases. In a similar study, Ogunesan *et al.* [24] modelled a bare flow of air with water and the behaviour of erosive particles in a pipe of 76.2 mm in diameter pipe. The superficial velocity of the gas phase was observed to range from a low of 0 . The rising velocity of the bubbles varied from 0.7 m/s to 40 m/s at maximum and rate of rise of the liquid phase remained constant at 0.3 m/s . The erosion aspect was examined when flow models were selected. The detailed outline of the integrated CFD-DPM model and the procedure for investigating material erosion within a 90° bend in a shale gas field under the conditions of gas-solid two-phase flow was first reported in the previous work presented by Peng *et al.* [25], The feasible k- ϵ turbulence, the discrete phase model and an erosion rate prediction model have been incorporated into this model. A new correlation was proposed, based on four dimensionless groups: Reynolds number, the ratio of the diameters of the two phases, the ratio of densities of two phases, and the number of drops in the continuous phase.

The model for long-term prediction of metal component deterioration, especially corrosion, is still a problem for potable water distribution systems. Pipe elbow joints are especially vulnerable to this sort of damage, which has caused considerable functional breakdowns with water pipelines [26]. Such degradation creates a significant risk which is why it is crucial to examine interventions of these components based on water flow, erosion, and corrosion [27].

Therefore, the aim of this study is to analyze the failure of 90° elbow joints in water pipelines due to erosion-corrosion. The water flow characteristics inside a 90° elbow are simulated using CFD in this work. The behavior of the water flow in terms of velocity profile. The Comparison of simulation results with the most degraded areas of 90° elbows was performed. Damage processes that have been observed in actual pipeline systems, such as cavitation, stress corrosion cracking (SCC), and erosion-corrosion, are greatly influenced by these parameters.

2. Materials and methods

2.1. Materials

The study's material is brass, more especially the Ba35 alloy, which has great mechanical qualities and high corrosion resistance and is frequently used in drinking water pipes. The chemical makeup of this alloy is depicted in Table 1 and includes minor amounts of alloying elements like iron (Fe) and lead (Pb) that assist in increasing the alloy's resistance to corrosion and erosion. Copper (Cu) makes up 65% of the alloy while zinc (Zn) makes up 35%. To assess this alloy's resilience in actual service settings, corrosion, and erosion tests were conducted on a sample of the material.

Table 1. Chemical composition of Ba35 brass alloy.

Element	Copper (Cu)	Zinc (Zn)	Lead (Pb)	Tin (Sn)	Iron (Fe)
Weight %	65.0	35.0	0.1	0.2	0.05

A 90° elbow constructed from the testing-use Ba35 alloy is depicted in Fig.1. In order to identify potential places for corrosion erosion damage, stress corrosion, and other types of degradation, this curve was put through a water flow simulation. It was feasible to track the velocity, pressure, and turbulence zones inside the bend using the numerical simulation model created under FLUENT. These elements are crucial in determining how quickly the material degrades.



Fig.1. Elbow fitting.

A chemical investigation of potable water conducted in this research sought to identify degradation effects which might occur in 90° elbow joints. The potable water obtained from the regional supply system has 49.7 ppm of calcium which causes moderate water hardness. A high ion concentration manifested through $683 \mu S cm^{-1}$ at 20°C reveals that electrochemical reactions at the metal surface are susceptible to this ion concentration. Dissolved oxygen reached 8.5 ppm which increases the risk of localized corrosion to occur mainly in turbulent flow areas. The measured water pH of 7.27 points toward mild neutrality thus reducing the risk of corrosive damage to severe extents. Trace elements including iron (Fe), manganese (Mn), zinc (Zn) and copper (Cu), fluoride (F) and lead (Pb) were identified in addition to other chemicals found in small amounts. The numerical simulations incorporated these material chemical traits to create more accurate predictions about service-specific material deterioration.

2.2. Mathematical Formulation

2.2.1. Governing equations

The flow analyzed in this paper is 3D continuous and turbulent while water is taken to be an incompressible fluid with constant properties. The descriptions of mass and momentum transport in such flow

processes are basic in modelling the dynamics of the system. These equations are widely used in CFD for the analysis of fluid flow and can be described as follows [26]:

Continuity equation:

$$\frac{\partial \rho}{\partial t} + \nabla(\rho v) = 0 \quad (2.1)$$

where:

- ρ is the fluid density,
- v is the velocity vector,
- ∇ denotes the divergence operator, which measures how much a field spreads out from a point.

This equation is to maintain the mass by calculating the change rate of the density with the divergence of the flow velocity field.

Momentum equation:

$$\frac{\partial}{\partial t}(\rho v) + \nabla(\rho v v) = -\nabla p + \nabla \tau \quad (2.2)$$

where:

- $\frac{\partial}{\partial t}(\rho v)$: The rate of change of momentum concerning time.
- $\nabla(\rho v v)$: The convective term, representing the transport of momentum due to the fluid's motion
- ∇p : The pressure gradient, which drives the flow.
- $\nabla \tau$: The divergence of stress tensor τ , which accounts for viscous forces.

The Navier Stokes momentum equation which is an application of Newton second law state that rate of change of momentum is equal to forces on the fluid. The other term on the right-hand side of the equation is pressure gradient and the viscous stress tensor τ indicating the shear stress within the fluid.

The Reynolds-averaged Navier-Stokes (*RANS*) equations also introduce extra unknowns, Reynolds stresses, to which a turbulence model is required to be applied. These equations also represent the basis of most of the CFD simulations used in engineering applications within the tropes of turbulent flows.

2.2.2. Turbulence Model: k - ε

To model the turbulence in the elbow joint, the standard k - ε model was employed. This model is widely used due to its balance between accuracy and computational cost. It solves two additional transport equations: one for the turbulent kinetic energy (k) and the other for the dissipation rate (ε). The equations are as follows:

Turbulent kinetic energy (k):

$$\frac{\partial k}{\partial t} + v \nabla k = G_k - \varepsilon \quad (2.3)$$

Here, G_k represents the production of turbulent kinetic energy due to mean velocity gradients.

Dissipation rate (ε):

$$\frac{\partial \varepsilon}{\partial t} + v \nabla \varepsilon = C_1 \frac{\varepsilon}{k} G_k - C_2 \frac{\varepsilon^2}{k} \quad (2.4)$$

where $C_1=1.44$ and $C_2=1.92$ are constants specific to the k - ε model, and the turbulent viscosity μ_t is determined by $\mu_t = C_u \frac{k^2}{\varepsilon}$ with $C_u = 0.09$.

Therefore, the k - ε model is more suitable for the f that contain fully developed turbulence and when the computational power is a limiting factor. It presents a workable compromise between accuracy, computational cost, and the reproduction of the fundamental characteristics of turbulence that are useful in common engineering applications such as pipelines.

2.2.3. Mathematical model and coupling of erosion and stress models

The essential procedure in this research is the mathematical modeling of erosion and mechanical stress coupling during erosion processes. Scientists used the discrete phase model (DPM) to simulate particle motions as well as impact and erosion processes through this expression:

$$\dot{E} = C_d f(\theta) \left(\frac{v_p}{v_{ref}} \right)^n, \quad (2.5)$$

- C_d is the erosion coefficient (material-dependent),
- $f(\theta)$ is an angular function accounting for the impact angle θ ,
- v_p is the velocity of the impacting particle,
- v_{ref} is a reference velocity,
- n is an empirical velocity exponent.

The coupling between the discrete phase (solid particles) and the mobile phase (fluid) is modeled using a two-way interaction approach. The key forces acting on the particles include:

Drag force exerted by the fluid on the particles:

$$F_d = \frac{1}{2} \alpha_d \rho_f A_p v_p^2, \quad (2.6)$$

- A_p is the projected area of the particle,
- α_d is the drag coefficient.

Lift force due to shear flow:

$$F_l = \frac{1}{2} \alpha_l \rho_f A_p v_p \times v, \quad (2.7)$$

- α_l is the lift coefficient,
- v is the velocity of the flow.

The quantitative aspect includes C_d as the material-specific erosion coefficient while the relationship between the impact angle and velocity of incoming particles appears in $f(\theta)$. The finite element analysis (FEA) included analysis of the fluid force applied to the elbow structure for localized stress determination. The strategy included a two-way coupling method to capture the bidirectional effects between fluid forces that modify structural stresses while structural stresses in turn affect fluid forces. The computational outcomes show the lowest radius area of the elbow generates maximal stress concentrations which matches with the highest erosion levels tracked by the CFD evaluation.

2.2.4. Structural stress model and fluid-structure interaction (FSI)

The force of the fluid on the elbow joint is considered in the structural analysis. The equilibrium equation governing the stress distribution within the solid material is:

$$\nabla \sigma + f = 0, \quad (2.8)$$

- σ is the Cauchy stress tensor,
- f represents the body forces acting on the structure.

The stress-strain relationship follows Hooke's law:

$$\sigma = D : \varepsilon, \quad (2.9)$$

- D is the elasticity matrix,
- ε is the strain tensor.

2.2.5. Coupling between structural stress and fluid flow

The fluid-structure interaction (FSI) approach ensures that the material internal stress equation is coupled with the flow equation. This is done through a two-way coupling mechanism where:

Shear stress from the fluid is applied to the solid domain:

$$\tau_w = \mu \frac{\partial v}{\partial n} /_{wall}, \quad (2.10)$$

- τ_w is the shear stress exerted by the fluid on the solid structure
- μ is the dynamic viscosity of the fluid,
- v is the velocity of the fluid,
- n is the normal direction to the wall (solid boundary).

Pressure loading exerted by the fluid on the structural surface is applied as:

$$p_w = p_f /_{interface}, \quad (2.11)$$

- p_w pressure applied on the solid wall due to the fluid,
- p_f is the fluid pressure at the interface.

The computed mechanical stress distribution confirms that regions of maximum erosion coincide with areas of peak structural stress, reinforcing the necessity of a coupled CFD-FEA simulation approach.

2.3. Numerical procedure with FLUENT

The section below describes the creation stage of elbow geometry along with the process of generating mesh and defining boundaries in a preprocessor called WORKBENCH-FLUENT.

2.3.1. Preprocessor: ANSYS WORKBENCH

The 3D model of 90° elbow was modeled and meshed in ANSYS WORKBENCH which is software specially developed to help analysts and engineers to model and mesh such geometries. Due to the bilateral nature of the studied problem, the computational region was limited to its half sizes to reduce computations, which did not affect the adequacy of modeling [28]. The elbow's geometry was based on creating a circular-section 90° joint and was modeled under typical conditions as prevailing in potable water distribution systems (Fig.2) [29].

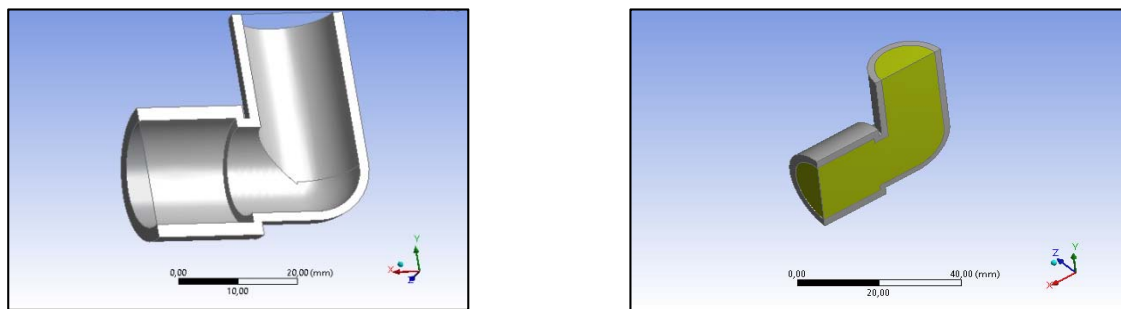


Fig.2. The geometry of the elbow joint under study.

2.3.2. Mesh generation

In order to maximize the match of the mesh with the physical geometry, the focus for mesh refinement was directed towards the walls of the elbow, where the interactions between the fluid and the walls are paramount [27]. A 3D tetrahedral mesh was used for the simulations and a denser mesh was applied near the wall where shear stress and flow behavior is expected to influence erosion and corrosion phenomena. Convergence of mesh independence was checked to confirm that, the results do not change with the mesh size. The meshing process was conducted in SYSTEMS ANSYS WORKBENCH while FLUENT was used as the solver. For the boundary layer, a finer grid was employed, because fluid velocities and gradients are very high at the boundary layer. Figure 3 displays the mesh that was produced for the elbow geometry together with the refinement at the wall boundaries.

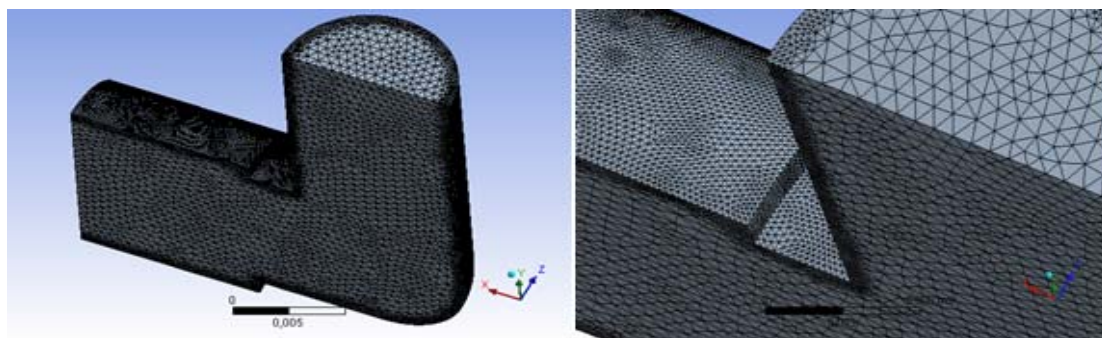


Fig.3. Meshing of the flow area.

Absolute control of unstructured tetrahedral meshing arose from the necessity to model flow separation and turbulence effects and localized erosion in the elbow section. The efficiency advantages of structured meshes clash with their inability to correctly model severe curvature shapes along with multi-directional velocity gradients appearing in *90-degree* elbow sections. An unstructured mesh delivered improved precision when it focused on areas with high shear stresses because these regions were prone to major erosion and corrosion. The current research did not require major structural deformations which made a moving mesh unnecessary since a fine fixed mesh maintained sufficient accuracy and stability. The chosen mesh configuration demonstrated reliability because a mesh independence test showed that velocity and pressure predictions together with erosion rates remained consistent when using meshes with more than 1.2 million elements regardless of increased complexity.

2.3.3. Boundary conditions

The simulation required three primary boundary conditions to accurately model the flow of water through the elbow joint (Tab.2): The simulation required three primary boundary conditions to accurately model the flow of water through the elbow joint:

- Pressure-inlet: At the inlet, there was an imposition of pressure of 7 bars. This pressure conducts typical service conditions of water pipelines in which the inlet pressure is more than the atmospheric pressure.
- Pressure-outlet: The outlet boundary condition was put as the pressure loading being the atmospheric pressure. Such a condition is explained by the fact that the water is discharged into an open system where pressure goes back to normal.
- Wall condition: The wall boundary condition which is a no-slip condition was applied on the walls of the elbow joint in the sense that the velocity of the fluid at the wall was zero concerning the wall. This condition describes the drag between the fluid passing through the internal surfaces of the elbow and is used in evaluating the erosion as well as the corrosion.

Table 2. Summary of the boundary conditions applied to the model.

Geometry	Boundary Condition
Inlet	Pressure-inlet = 7 bar
Outlet	Pressure-outlet = P_{atm}
Wall boundary condition	No-slip wall condition

These boundary conditions help in achieving a proper emulation of flow conditions in water pipelines and hence estimating the flow-induced damage mechanisms such as cavitation, turbulence, impact velocity, etc.

3. Results and discussion

The discussions of the results of the simulation of the 90° elbow joint are presented in this section. The main features analyzed are pressure distribution, velocity distribution, and eroded rates on the different areas of the joint elbow.

3.1. Pressure profiles

Figure 4 shows the static pressure contours and static pressure profiles as calculated and analyzed using the simulation. The following observations can be made based on these results:

The upstream pressure, before the elbow joint, is relatively high and practically constant in all sections that make up the joint. This high pressure is explained by the fact that the liquid experiences a few resistances when it comes to the bended portion of the elbow [30].

Regarding the pressure drop across the elbow, it is evident that a pressure drop happens as the fluid flows into the pipe and after that through the shaped elbow. This change in direction results in a decrease in

pressure, probably due to the increase in flow rate and the change in the fluid trajectory. This phenomenon is particularly observable near the walls, where the liquid comes into contact, causing a local variation in pressure.

Finally, cavitation zones shape close the inner walls of the elbow, coming about in low-pressure zones. Cavitation happens when fluid passes through these low-pressure regions, causing vapor bubbles to make and collapse as they enter high-pressure locales. This process can essentially influence the surface and lead to fabric disappointment within the long term.

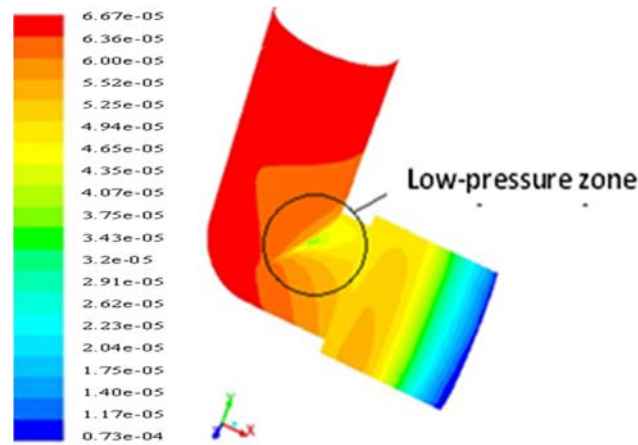


Fig.4. Pressure contours.

The pressure contours on the elbow part represent clearly that the most vulnerable regions exposed to cavitation and surface erosion problematics are in the region of the bend of the elbow part having the maximum pressure drop. These zones are of considerable importance in the evaluation of the possible erosion and corrosion threats.

3.2. Velocity profiles

The fluid velocity profiles shown in Fig.5 show the rise in the flow velocity within the elbow region. This will keep the velocity of the fluid flowing through an elbow pipe continuously high, especially around the outer periphery of the elbow. Of course, this acceleration is due to the curvature that imparts redistribution to the flow. The maximum velocities are attained just near the outlet and right after the place where the pipe diameter has increased due to the presence of the elbow.

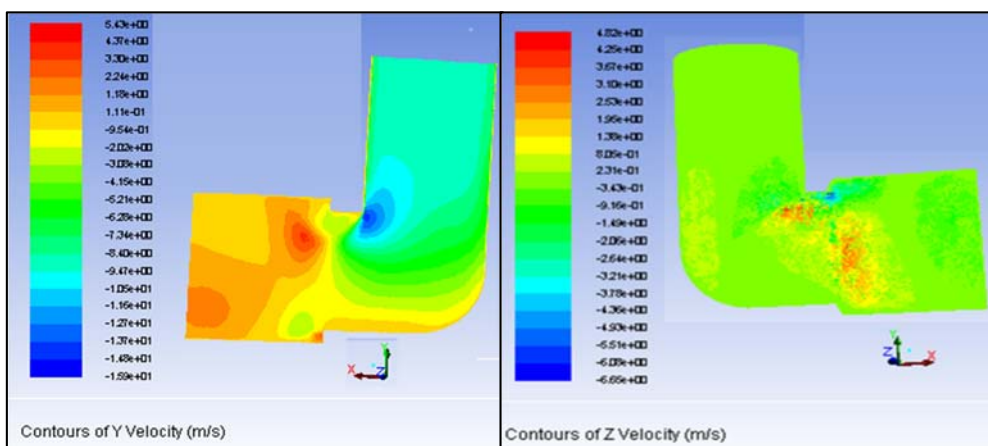


Fig.5. Contours of Y and Z velocity.

Vortices and flow separation with associated recirculation zones will set in at the inner radius of the elbow. Within these areas, the fluid rotates upon itself while forming a local swirl. Instabilities of the flow may interfere with protective film formation on the outer face of the elbow and thus may increase erosion and material degradation [29].

In the case of the elbow geometry, the contours of velocity determined indicate that there are high variations in both velocity and turbulence within the flow field. Therefore this aspect should not be used alone in the determination of the elbow's life under operations but with some consideration of operations.

3.3. Erosion rate: DPM

To predict the erosion rate, the use of DPM in elbow joints was used in this experimental study. The topography of the erosion rate is represented by the contours shown in Fig.6. The contours of the erosion rate on the elbow surface are indicated.

It was observed that the areas with the highest erosion rates are located in the lower radius area of the elbow. These are the areas where the fluid approaches and hits the surface at the highest velocity, thus causing more wear over time. The maximum erosion rate in the current implementation is $6.5 \times 10^{-3} \text{ kg}/(\text{m}^2 \cdot \text{s})$, which means that long-term material degradation is most likely in this region.

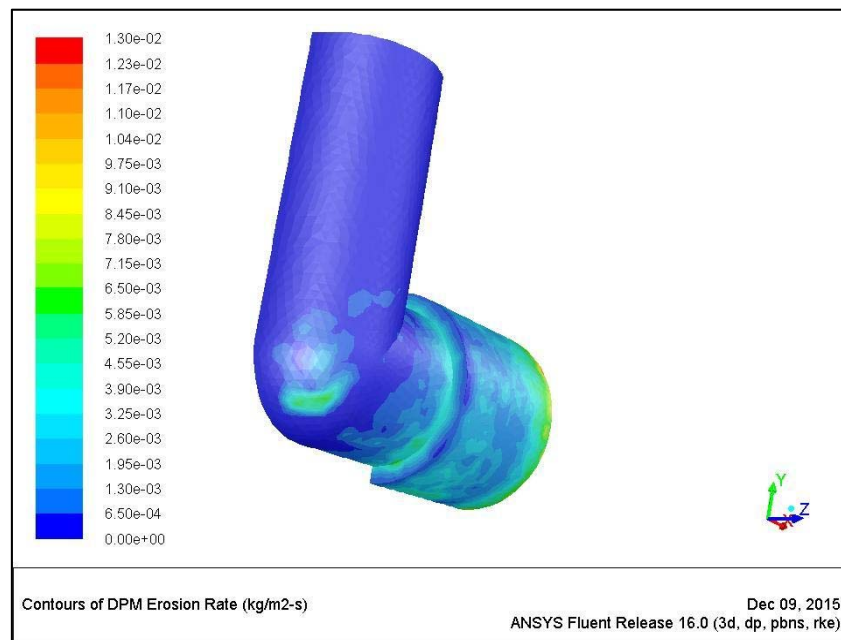


Fig.6. Contours of erosion rate.

Based on the averaged results presented above, it is evident that over time the elbow joint will experience considerable material erosion in areas experiencing high-velocity flow and turbulence. This erosion is even made worse by the fact that the fluid contains solid particles that cause the wear process to occur at a much faster rate.

3.4. Fluid-structure interaction (FSI)

Besides fluid dynamics evaluation, the CFD analysis of fluid-structure interaction (FSI) was carried out to investigate the influence of the flow forces on the structural behavior of the elbow joint. The wall pressures that were computed from the fluid-structure interaction simulation were exported and used as loading

on the structural simulation completed in ANSYS. This made it possible to determine the stress experienced on the walls of the elbow by both the pressure of the fluid as well as mechanical forces.

The contours of the equivalent stress due to the pressure field are revealed in the Fig.7. It was observed that the parts exposed to the greatest degree of mechanical stress are eroded more severely, and areas at the lower radius of the elbow are most severely eroded. The stress level up to which these zones are most susceptible to structural deformation and failure with time was found to be approximately 775 MPa (Fig.7).

Because of the loose crevices along the flanks of the bending of the pipe, the elbow will be subjected to stress corrosion cracking (SCC) from mechanical stress from the fluid flow coupled with corrosion from water. This form of degradation can cause the formation of cracks in regions whereby the structural material is compromised with stress as well as erosion.

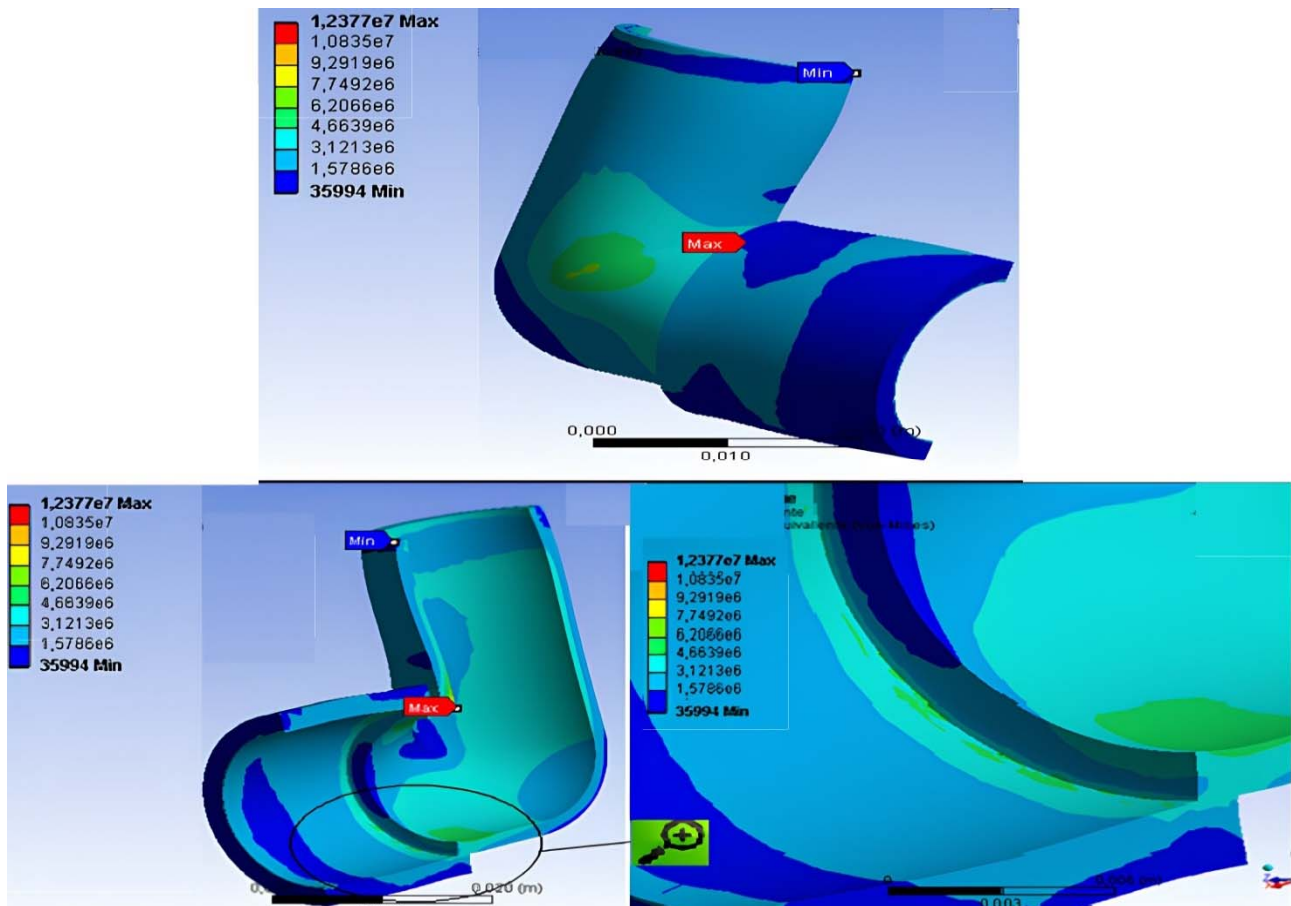


Fig.7. Equivalent stresses resulting from the applied pressure field.

The fluid-structure interaction (FSI) analysis explores the dual influence of hydrodynamic forces together with mechanical stresses that affect the elbow joint. The elbow joint deals with two key types of loading mechanisms: fluid-induced shear forces and cyclic mechanical stresses which arise from pressure fluctuations and turbulent vortices as well as particle-wall interactions. The combination of these elements functions as important agents that speed up material deterioration of elbow structures. Results showed that maximum mechanical stresses observed precisely at sites where erosion occurred according to Fig.8 data. Researchers have studied how flow-induced forces modify structural stress patterns to show that specific mechanical forces increase stress corrosion cracking (SCC) formation rates thus shortening material lifespan.

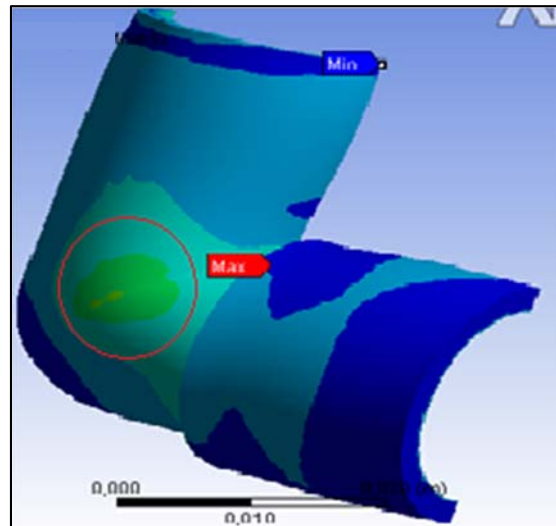


Fig.8. Comparison of simulation results with the most degraded areas of 90° elbows.

The simulation results presented in this work clearly reveal that the 90° elbow joint experiences high mechanical stress resulting from velocity, pressure, and turbulence. Such factors lead to the erosion and corrosion of materials in use thus contributing to material degradation.

Regarding the issue of pressure loss and cavitation, the pressure distribution of the simulations highlights very frequent pressure oscillations. This indicates a possibility of cavitation formation on the surface of the elbow layer, especially at distances from the wall of the curved intersection. If this effect is not taken into account at the design stage, it can lead to surface wear and even failure.

Regarding speed and erosion, note the high speeds on the outer wall of the elbow and therefore high erosion rates. In addition, the presence of significant recirculation and turbulence zones is sometimes considered an aggravating factor, as these conditions hinder the formation of regular protective layers on the surface. Finally, with regard to structural integrity, the combined effects of pressure, velocity and erosive forces cause accelerated degradation of the assembled elbow. Although no changes to the design or maintenance program are anticipated, this can lead to structural failure after several years of service.

The consequences of erosive flow for the geometry of the elbow joint were considered during the preliminary study, and the influence of the flow and particle parameters on the arrangement was examined in the framework of the parametric study. The effects of change in particle injection velocities (2.5 m/s , 5 m/s , and 7.5 m/s) and particle size from $10\ \mu\text{m}$ to $200\ \mu\text{m}$ were also explored in this study. It was assumed that particles are spherical and the impact is normal to the elbow surface, which is close to the reality in the steady flow with dispersed particles.

This is a parametric study that sheds insight into the tendency of erosion under various flow conditions and characteristics of particles. Effects due to these parameters are significant in deciding the wearing off of the elbow and therefore, these parameters must be well controlled from the design phase up to the operation phase of pipeline systems.

The dependency of the maximum erosion rate as a function of the particle size for the three tested velocities is illustrated in the Fig.9. It was found that increasing speed influences the regression parameters, in the sense that the erosion rate increases with particle size, regardless of the speed regime studied. This is so since particles that has large dimensions possess more kinetic energy, and thus impact forces in contact surfaces of the elbow. For the particle size of below $50\ \mu\text{m}$, the raise of the erosion rate is little. However, if the area exceeds this size, then there is an increase in the erosion rate particularly for the higher velocities of the droplets.

It has also been observed that there are large differences in erosive effects depending on the flow velocity. Hence at the minimum velocity of movement, or 2.5 m/s , the erosion rates are generally low for all the particle sizes. However, they become as the velocity increases to 5 m/s and 7.5 m/s . The erosion rate

increases steeply at a flow velocity of 5 m/s, especially for the larger-sized particles. For instance, at 7.5 m/s, the increase of the particles' size to 10 μm results in a rather significant increase in the erosion rate.

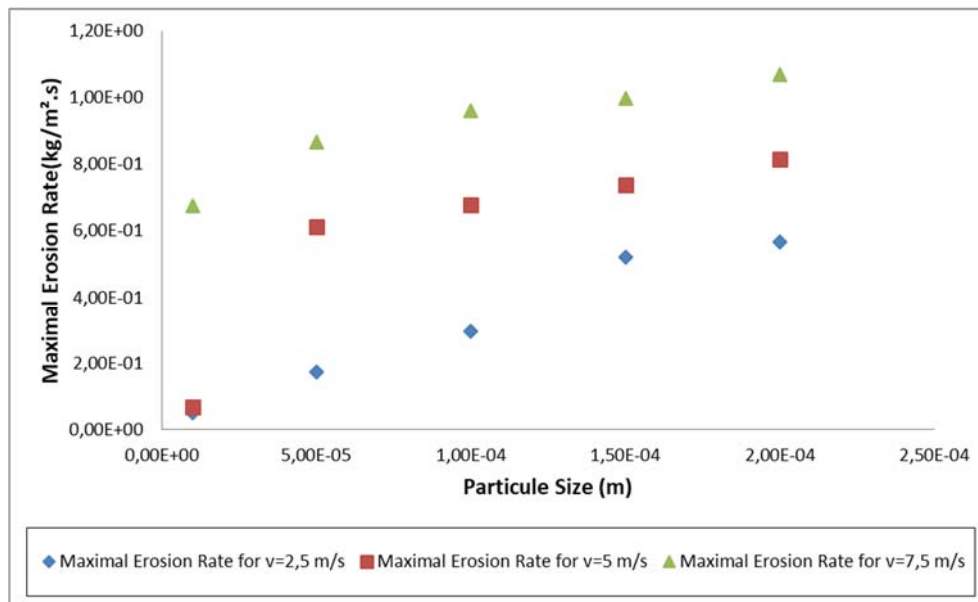


Fig.9. Variation of the maximum erosion rate as a function of particle sizes for different velocities.

This parametric analysis shows that velocity is a very influential factor to the degree of erosion in the elbow joint besides the particle size. If it is to be applied practically, one may want to maintain control of the particle size distribution and also try controlling flow velocities wherever possible to address this issue of material degradation in such systems.

The parametric study reveals several important insights into the factors influencing erosion in 90° elbow joints:

- Critical impact of particle size: larger particles result in higher erosion rates since these particles possess higher energy or momenta when they impact the surface. Systems that cater to pipeline means involving the flow of liquids that have large particles in suspension must provide for this or else ensure that the pipeline elbows are made from stronger material.
- Velocity thresholds: From the above data the differences that exist between erosion values with the increase in flow velocity signify that there are velocities beyond which erosions become critical. Elbow joints are one of the most critical pipeline components and thus for pipeline designers, it can help to prolong the life of this element by avoiding the velocities that are rising above such thresholds.
- Erosion mitigation strategies: taking into account these outcomes, it is possible to reduce or even eliminate the process of erosion through the decrease of velocity of a fluid and the elimination of coarse particles that are present in a fluid. Observation and analysis of particle size in the fluid will probably assist in setting proper operation parameters to reduce wear on the particles.
- The integration of CFD simulations with parametric studies provides an able means of examining and predicting erosion in intricate flow systems such as elbow junctions. The analyses shown here can be applied to enhance the methodology and management for the pipeline, helping to increase working lifetimes and minimize the chances of failure.

4. Conclusions

In this paper, a detailed numerical modelling for the behavior of water flow in a 90° elbow joint of a potable water pipeline was conducted. Through the CFD analysis using FLUENT we further ran several

parametric studies to predict the sensitivity to the flow parameters such as velocity profile pressure distribution and turbulent zones in triggering material degradative conditions at the elbow joint. The results therefore showed that the elbow is the most vulnerable to erosion and cavitation where high velocity and pressure gradients are probably the greatest.

The simulation results show that:

- High-pressure gradients, especially on steep slopes, favor cavity formation and surface wear.
- High velocity near the outer elbow wall severely erodes this area, with more accentuated erosive effects from solid particles suspended in the fluid.
- Disruptions through the recirculation loops prevent the establishment of a protective layer, consequently leading to material degradation.
- DPM was used to evaluate the erosion rate, and the lower radius of the elbow was found to be the most affected region, with the maximum erosion rate of $6.5 \times 10^{-3} \text{ kg} / (\text{m}^2\text{s})$.
- Fluid-structure interaction (FSI) analysis revealed that with maximum mechanical stresses of 775 MPa, the erosion and crack initiation by stress corrosion was favored.
- The parametric study indicated that increased fluid velocity and particle size increase the rate of erosion, particle sizes exceeding 50 μm and speeds up to 7.5 m/s in particular.

Future work should focus on the experimental validation of CFD outcomes in real-world conditions, investigate alternative elbow geometries to mitigate erosion and cavitation, choose advanced materials that exhibit resistance to corrosion and erosion, and integrate fluid-structure interaction (FSI) to assess mechanical loads and stress corrosion. This will enhance pipeline durability.

Nomenclature

CFD – computational fluid dynamics.

Ba35 – brass alloy containing 65% copper (Cu) and 35% zinc (Zn).

FSI – integrate fluid-structure interaction.

DPM – discrete phase model.

SCC – stress corrosion cracking.

RANS – Reynolds-averaged Navier-Stokes.

3D – three-dimensional.

References

- [1] Aguirre J., Walczak M. and Rohwerder M. (2019): *The mechanism of erosion-corrosion of API X65 steel under turbulent slurry flow: Effect of nominal flow velocity and oxygen content.*– Wear, vol.438, p.203053, <https://doi.org/10.1016/j.wear.2019.203053>.
- [2] Wang Z. and Zheng Y. (2021): *Critical flow velocity phenomenon in erosion-corrosion of pipelines: Determination methods, mechanisms and applications.*– Journal of Pipeline Science and Engineering, vol.1, No.1, pp.63-73, <https://doi.org/10.1016/j.jpse.2021.01.005>.
- [3] Ayyagari A., Hasannaemi V., Grewal H.S., Arora H. and Mukherjee S. (2018): *Corrosion, erosion and wear behavior of complex concentrated alloys: A review.*– Metals, vol.8, No.8, p.603, <https://doi.org/10.3390/met8080603>.
- [4] Khan R., Wieczorowski M., Seikh A.H. and Alnaser I.A. (2024): *Experimental and numerical study of erosive wear of t-pipes in multiphase flow.*– Engineering Science and Technology, an International Journal, vol.52, p.101683, <https://doi.org/10.1016/j.jestch.2024.101683>.
- [5] Shrestha R., Gurung P., Chitrakar S., Thapa B., Neopane H. P. Guo Z. and Qian Z. (2024): *Review on experimental investigation of sediment erosion in hydraulic turbines.*– Frontiers in Mechanical Engineering, vol.10, p.1526120, <https://doi.org/10.3389/fimech.2024.1526120>.
- [6] Elemuren R., Tamsaki A., Evitts R., Oguocha I.N., Kennell G., Gerspacher R. and Odeshi A. (2019): *Erosion-corrosion of 90 AISI 1018 steel elbows in potash slurry: Effect of particle concentration on surface roughness.*– Wear, vol.410, pp.149-155, <https://doi.org/10.1016/j.wear.2019.04.014>.

- [7] Zeng L., Zhang G. and Guo X. (2014): *Erosion-corrosion at different locations of X65 carbon steel elbow.*– Corrosion Science, vol.85, pp.318-330, <https://doi.org/10.1016/j.corsci.2014.04.045>.
- [8] Owen J., Ducker E., Huggan M., Ramsey C., Neville A. and Barker R. (2019): *Design of an elbow for integrated gravimetric, electrochemical and acoustic emission measurements in erosion-corrosion pipe flow environments.*– Wear, vol.428, pp.76-84, <https://doi.org/10.1016/j.wear.2019.03.010>.
- [9] Kesana N., Grubb S., Mclaury B. and Shirazi S. (2013): *Ultrasonic measurement of multiphase flow erosion patterns in a standard elbow.*– Journal of Energy Resources Technology, vol.135, No.3, p.032905, <https://doi.org/10.1115/1.4023331>.
- [10] Vieira R.E., Parsi M., Zahedi P., Mclaury B.S. and Shirazi S.A. (2017): *Sand erosion measurements under multiphase annular flow conditions in a horizontal-horizontal elbow.*– Powder Technology, vol.320, pp.625-636, <https://doi.org/10.1016/j.powtec.2017.07.087>.
- [11] Parsi M., Kara M., Agrawal M., Kesana N., Jatale A., Sharma P. and Shirazi S. (2017): *CFD simulation of sand particle erosion under multiphase flow conditions.*– Wear, vol.376, pp.1176-1184, <https://doi.org/10.1016/j.wear.2016.12.021>.
- [12] Parsi M., Najmi K., Najafifard F., Hassani S., Mclaury B.S. and Shirazi S.A. (2014): *A comprehensive review of solid particle erosion modeling for oil and gas wells and pipelines applications.*– Journal of Natural Gas Science and Engineering, vol.21, pp.850-873, <https://doi.org/10.1016/j.jngse.2014.10.001>.
- [13] Kang R. and Liu H. (2020): *An integrated model of predicting sand erosion in elbows for multiphase flows.*– Powder Technology, vol.366, pp.508-519, <https://doi.org/10.1016/j.powtec.2020.02.072>.
- [14] Farokhipour A., Mansoori Z., Saffar-Avval M. and Ahmadi G. (2020): *3D computational modeling of sand erosion in gas-liquid-particle multiphase annular flows in bends.*– Wear, vol.450, p. 203241, <https://doi.org/10.1016/j.wear.2020.203241>.
- [15] Zhu H., Lin Y., Zeng D., Zhou Y., Xie J. and Wu Y. (2012): *Numerical analysis of flow erosion on drill pipe in gas drilling.*– Engineering Failure Analysis, vol.22, pp.83-89, <https://doi.org/10.1016/j.engfailanal.2012.01.007>.
- [16] Yang X., Xi T., Qin Y., Zhang H. and Wang, Y. (2024): *Computational fluid dynamics-discrete phase method simulations in process engineering: a review of recent progress.*– Applied Sciences, vol.14, No.9, p.3856, <https://doi.org/10.3390/app14093856>.
- [17] Haider R., Li X., Shi W., Lin Z., Xiao Q. and Zhao H. (2024): *Review of computational fluid dynamics in the design of floating offshore wind turbines.*– Energies, vol.17, No.17, p.4269, <https://doi.org/10.3390/en17174269>.
- [18] Alghurabi A., Mohyaldinn M., Jufar S., Younis O., Abduljabbar A. and Azuwan M. (2021): *CFD numerical simulation of standalone sand screen erosion due to gas-sand flow.*– Journal of Natural Gas Science and Engineering, vol.85, p.103706, <https://doi.org/10.1016/j.jngse.2020.103706>.
- [19] Barile C., Casavola C. and De Cillis F. (2018): *Mechanical comparison of new composite materials for aerospace applications.*– Composites Part B: Engineering, vol.162, pp.122-128, <https://doi.org/10.1016/j.compositesb.2018.10.101>.
- [20] Duarte C.A.R. and de Souza F.J. (2017): *Innovative pipe wall design to mitigate elbow erosion: A CFD analysis.*– Wear, vol.380, pp.176-190, <https://doi.org/10.1016/j.wear.2017.03.015>.
- [21] Peng W., Cao X., Hou J., Ma L., Wang P. and Miao Y. (2021): *Numerical prediction of solid particle erosion under upward multiphase annular flow in vertical pipe bends.*– International Journal of Pressure Vessels and Piping, vol.192, p.104427, <https://doi.org/10.1016/j.ijpvp.2021.104427>.
- [22] Ejeh C.J., Boah E.A., Akhabue G.P., Onyekperem C.C., Anachuna J.I. and Agyebi I. (2020): *Computational fluid dynamic analysis for investigating the influence of pipe curvature on erosion rate prediction during crude oil production.*– Experimental and Computational Multiphase Flow, vol.2, No.4, pp.255-272, <https://doi.org/10.1007/s42757-019-0055-5>.
- [23] Lain S. and Sommerfeld M. (2019): *Numerical prediction of particle erosion of pipe bends.*– Advanced Powder Technology, vol.30, No.2, pp.366-383, <https://doi.org/10.1016/j.apt.2018.11.014>.
- [24] Ogunesan O.A., Hossain M., Iyi D. and Dhroubi M.G. (2019): *CFD modelling of pipe erosion due to sand transport.*– In Proceedings of the 1st International Conference on Numerical Modelling in Engineering, vol.2, Ghent University, Springer, pp.274-289, https://doi.org/10.1007/978-981-13-2273-0_22.
- [25] Peng S., Chen Q., Shan C. and Wang D. (2019): *Numerical analysis of particle erosion in the rectifying plate system during shale gas extraction.*– Energy Science & Engineering, vol.7, No.5, pp.1838-1851, <https://doi.org/10.1002/ese3.395>.
- [26] Wang W., Sun Y., Wang B., Dong M. and Chen Y. (2022): *Influence of sand fines transport velocity on erosion-corrosion phenomena of carbon steel 90-degree elbow.*– Metals, vol.10, No.5, p.626, <https://doi.org/10.3390/met10050626>.

- [27] Wang W., Sun Y., Wang B., Dong M. and Chen Y. (2022): *CFD-based erosion and corrosion modeling of a pipeline with CO₂-containing gas-water two-phase flow.*– Energies, vol.15, No.5, p.1694, <https://doi.org/10.3390/en15051694>.
- [28] Abuhatira A.A., Salim S.M. and Vorstius J.B. (2023): *CFD-FEA based model to predict leak-points in a 90-degree pipe elbow.*– Engineering with Computers, vol.39, No.6, pp.3941-3954, <https://doi.org/10.1007/s00366-023-01853-4>.
- [29] Hong B., Li X., Li Y., Yu Y., Wang Y., Gong J. and Ai D. (2021): *Numerical simulation of elbow erosion in shale gas fields under gas-solid two-phase flow.*– Energies, vol.14, No.13, p.3804, <https://doi.org/10.3390/en14133804>.
- [30] Edwards J.K., McLaury B.S. and Shirazi S.A. (2001): *Modeling solid particle erosion in elbows and plugged tees.*– Journal of Energy Resources Technology, vol.123, No.4, pp.277-284, <https://doi.org/10.1115/1.1413773>.

Received: January 7, 2025

Revised: April 7, 2025